Metal nanoparticles in strongly confined beams: transmission, reflection and absorption

Nassiredin M. Mojarad nassiredin.mojarad@phys.chem.ethz.ch Laboratory of Physical Chemistry, ETH Zurich, 8093 Zurich, Switzerland

Gert Zumofen gert.zumofen@phys.chem.ethz.ch Laboratory of Physical Chemistry, ETH Zurich, 8093 Zurich, Switzerland

Vahid Sandoghdar vahid.sandoghdar@ethz.ch Laboratory of Physical Chemistry, ETH Zurich, 8093 Zurich, Switzerland

Mario Agio mario.agio@phys.chem.ethz.ch Laboratory of Physical Chemistry, ETH Zurich, 8093 Zurich, Switzerland

We investigate the interaction of tightly focused light with the surface-plasmon-polariton resonances of metal nanospheres. In particular, we compute the scattering and absorption ratios as well as transmission and reflection coefficients. Inspired by our previous work in [1], we discuss how well a metal nanoparticle approximates a point-like dipolar radiator. We find that a 100 nm silver nanosphere is very close to such an ideal oscillator. Our results have immediate implications for single nanoparticle spectroscopy and microscopy as well as plasmonics. [DOI: 10.2971/jeos.2009.09014]

Keywords: metal nanoparticles, focused light, surface plasmon-polaritons, scattering and absorption

1 INTRODUCTION

The use of tightly focused light to investigate individual nano-objects has received a renewed attention from both the theoretical [1]–[6] and the experimental points of view [7]–[17]. The driving idea is to improve light-matter interaction without the need for an optical cavity and to explore the detection limits of very small material bodies in free space. Promising results and applications have been reported for instance in ultra-sensitive label-free detection of biological samples [12], spectroscopy of very small gold nanoparticles (NPs) [7]–[11], and of single quantum emitters [13]–[18].

We have recently shown that a point-like oscillating dipole strongly attenuates a tightly confined beam incident on it [1]. In particular, we have found that a focused plane wave (FPW) can be reflected by up to 85%. These results are valid for a classical radiator as well as for a two-level system under weak excitation. Experiments to confirm these theoretical findings are difficult to perform on quantum emitters for several reasons. For example, in the solid state they should be cooled down to cryogenic temperatures [13]–[17], where high-NA optics is difficult to use. On the other hand, handling single atoms in vacuo is difficult because they must be trapped and kept in the focal spot [17]. Here we show that one could think of replacing the quantum emitter with a mesoscopic system that has the properties of an oscillating dipole.

Metal NPs have optical properties analogous to a dipolar oscillator. They exhibit distinct resonances even if their size is smaller than the incident wavelength because of the excitation of surface plasmon-polaritons [19]. In fact, we have recently performed experiments where gold NPs were used to investigate fundamental physical problems related to classical and quantum oscillators close to neutral bodies or interacting with each others [20, 21].

Metal NPs, specifically gold and silver, have been studied under tight illumination and their plasmon-polariton spectra have been discussed for different focusing angles both in the near- and far-field regimes [3]. It was shown that higher-order modes are not excited when the incident light is tightly focused. On the other hand, it turns out that the scattering efficiency at the dipolar resonance is close to the value for plane-wave illumination. This quantity is the ratio between the scattering cross section and the cross sectional area of the NP and compares the electromagnetic size with the geometrical size of the NP [19]. Because in a tight focus the intensity is strongly position and polarization dependent, it is more instructive to adopt another definition for the scattering efficiency, namely the scattered power divided by the incident power [1, 22]. This quantity, which we call *scattering ratio*, is relevant because, as we will see, it is directly related to the transmission of light through the NP and can be compared with the result for a point-like oscillating dipole. Furthermore, it provides information on the detection limits of very small NPs and on the efficiency of light absorption. For instance, since the background noise is proportional to the incident power, increasing the scattering ratio leads to a better signal.

In this paper we want to focus our attention on the dipolar resonance and see how well metal NPs behave as point-like dipolar radiators. Moreover, by computing transmission and reflection we explore the detection limits for very small NPs

Received January 28, 2008; published April 10, 2009 ISSN 1990-2573

and investigate their potential as light absorbers. While these topics belong to the basics of light scattering [19], the treatment of tightly focused light and power ratios in place of cross sections addresses questions of current interest.

2 RESULTS AND DISCUSSION

2.1 Generalized Mie theory

The problem we want to tackle is a nano-object illuminated by a plane wave polarized along x and focused by an aplanatic system [1, 3, 23] as shown in the inset of Figure 1. The focused beam can be expressed using the multipole expansion

$$\mathbf{E}_{\text{inc}} = \sum_l A_l \left(\mathbf{N}^{(1)}_{e1l} - i\mathbf{M}^{(1)}_{o1l} \right), \tag{1}$$

where l runs from 1 to infinity, and $\mathbf{N}^{(1)}_{e1l}$, $\mathbf{M}^{(1)}_{o1l}$ are respectively the transverse magnetic and transverse electric multipoles according to the notation of [19]. A_l are the expansion coefficients [3, 24]

$$A_l = (-i)^l E_0 k f \frac{2l+1}{2l^2(l+1)^2} \times \int_0^{\alpha} a(\theta) \left[\frac{P^1_l(\cos\theta)}{\sin\theta} + \frac{\mathrm{d}P^1_l(\cos\theta)}{\mathrm{d}\theta} \right] \sin\theta \mathrm{d}\theta, \tag{2}$$

where E_0 is the amplitude of the incident electric field, f is the focal length of the lens, k is the wavevector and $a(\theta) = \sqrt{\cos\theta}$ is the apodization function for an aplanatic system [23]. $P^1_l(\cos\theta)$ are the associated Legendre functions of the first kind, with degree l and order 1 [19]. Note that the focusing angle α is the only parameter that dictates the relative weight $|A_l / A_1|$.

In the next step a sphere is placed at the focus. The scattered field $\mathbf{E}_{\text{sca}}$ can be found by matching the boundary conditions at its surface

$$\mathbf{E}_{\text{sca}} = \sum_l A_l \left(-a_l \mathbf{N}^{(3)}_{e1l} + i b_l \mathbf{M}^{(3)}_{o1l} \right), \tag{3}$$

where a_l and b_l are the Mie coefficients [3, 19]. The superscript (3) in place of (1) in $\mathbf{N}_{e1l}$ and $\mathbf{M}_{o1l}$ specifies that the multipoles contain only outgoing waves instead of outgoing and incoming ones. As soon as the incident and scattered fields are determined, the scattered power (P_{sca}) and the sum of scattered and absorbed powers ($P_{\text{s+a}}$) are calculated by respectively integrating the Poynting vectors of the scattered field and of the interference term over the entire space. Using the properties of multipoles, analytical expressions for P_{sca} and $P_{\text{s+a}}$ are found to be [3]

$$P_{\text{sca}} = \frac{\pi}{2Zk^2} \sum_l \frac{2l^2(l+1)^2}{2l+1} |A_l|^2 \left(|a_l|^2 + |b_l|^2 \right), \tag{4}$$

$$P_{\text{s+a}} = \frac{\pi}{2Zk^2} \sum_l \frac{2l^2(l+1)^2}{2l+1} |A_l|^2 \,\mathrm{Re}\{a_l + b_l\}, \tag{5}$$

where Z is the impedance in the background medium. Note that Eq. (5) is the textbook formula for the extinction [19], but $P_{\text{s+a}}$ does not represent the power removed from the incident beam in a transmission experiment, because for focused illumination the optical theorem is not valid [25]. We discuss this point in Section 2.3, where we consider the problem of transmission and reflection. The absorbed power is defined as usual by $P_{\text{abs}} = P_{\text{s+a}} - P_{\text{sca}}$.

2.2 Scattering and absorption ratios

Contrary to a plane wave, a beam carries a finite amount of power. Thus, we can quantify the response of our nano-object by considering the scattering ($\mathcal{K}_{\text{sca}}$) and absorption ($\mathcal{K}_{\text{abs}}$) ratios that are defined by dividing P_{sca} and P_{abs} respectively by the total incident power P_{inc} [1, 22],

$$P_{\text{inc}} = f^2 \int_0^{2\pi} \int_{\pi/2}^{\pi} \mathbf{S}_{\text{inc}} \cdot \mathbf{n} \, \sin\theta \, \mathrm{d}\theta \, \mathrm{d}\phi, \tag{6}$$

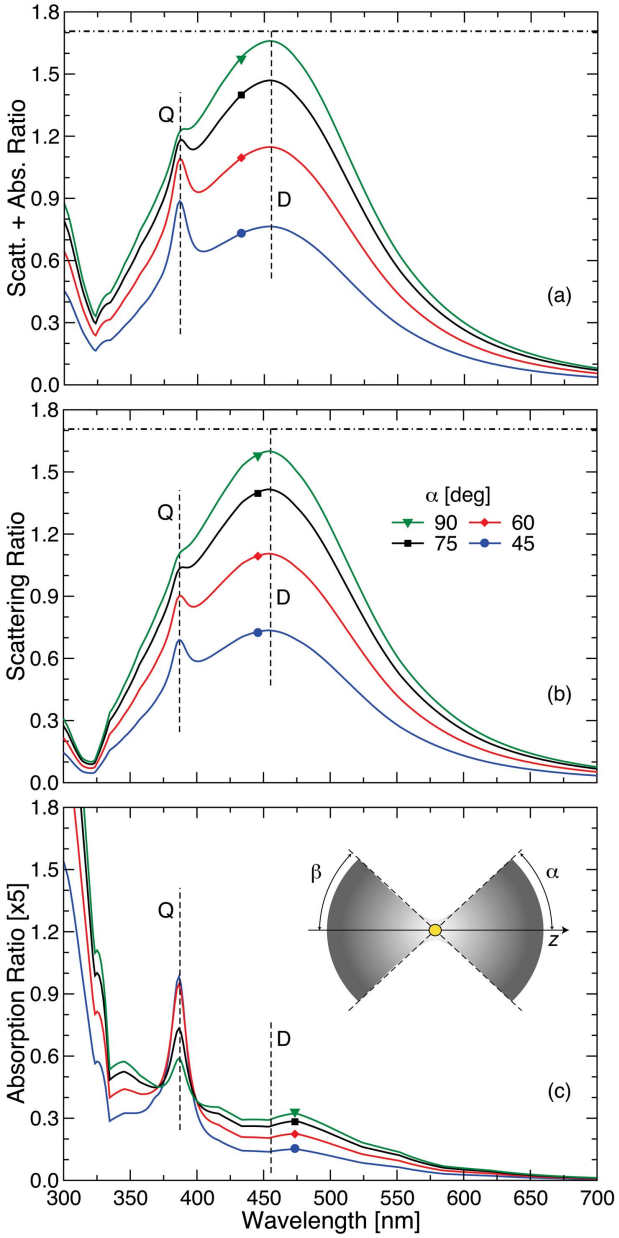

FIG. 1 (a) Scattering plus absorption $\mathcal{K}_{\text{s+a}}$, (b) scattering $\mathcal{K}_{\text{sca}}$ and (c) absorption $\mathcal{K}_{\text{abs}}$ ratios for a 100 nm silver NP in water ($n_b = 1.3$) under a FPW for different focusing angles α. The collection angle is $\beta = 180°$. The dashed-dotted lines in (a) and (b) refer to $\mathcal{K}_{\text{sca}}$ for a resonant point-like oscillating dipole for $\alpha = 90°$ [1]. The vertical dashed lines mark the dipole D and quadrupole Q resonances. $\mathcal{K}_{\text{abs}}$ is multiplied by a factor of 5 for clarity. The inset in (c) shows a NP in a focused beam, indicating the focusing angle α, the collection angle β, and the optical axis z.

where $\mathbf{S}_{\rm inc}$ is the Poynting vector of the incident field taken in the far field at f and $\mathbf{n}$ is the unit vector normal to the spherical wave-front. For completeness, we also define the quantity $\mathcal{K}_{\rm s+a} = P_{\rm s+a}/P_{\rm inc}$. We focus our attention on silver and gold NPs because they exhibit a strong resonant behavior in the visible spectral range. The NPs are in a homogeneous background medium with index of refraction $n_{\rm b} = 1.3$ (immersion in water).

Figure 1 displays $\mathcal{K}_{\rm s+a}$, $\mathcal{K}_{\rm sca}$ and $\mathrm{K}_{\rm abs}$ for a 100 nm silver NP at different focusing angles. Tighter focusing has two major effects. First, the efficiency increases and reaches the maximum value for $\alpha = 90^\circ$. Second, a stronger focus reduces the coupling to higher order multipoles because they have a small contribution in the incident field [3]. As a consequence, $\mathcal{K}_{\rm abs}$ decreases at the quadrupole (Q) resonance if α increases. The fact that $\mathcal{K}_{\rm s+a}$ and $\mathcal{K}_{\rm sca}$ can exceed 1 does not violate the conservation of energy since $P_{\rm sca}$ and $P_{\rm s+a}$ contribute to the energy balance with opposite signs [19] and their sum never exceeds $P_{\rm inc}$ [1].

A small metal NP is often treated using a dipolar polarizability

$$\alpha_{\rm NP} = \frac{\alpha_\circ}{1 - i\frac{k^3}{6\pi}\alpha_\circ}, \tag{7}$$

where $\alpha_\circ$ is the NP electrostatic polarizability [19, 26]. Eq. (7) shows that $\alpha_{\rm NP}$ approaches the value of a classical oscillator on resonance [1, 27] only if $\alpha_\circ \gg 6\pi/k^3$. This occurs if the absorption losses are negligible with respect to radiation, irrespective of the magnitude of $\alpha_\circ$, or if $\alpha_\circ$ is large because of the NP size. In the first case, the losses can be reduced by choosing the material composing the NP, or by changing the background index and the NP shape to shift the resonance [19]. In the second case, the size of the NP cannot be too large because higher-order resonances begin to spectrally overlap with the dipolar one and depolarization effects become stronger [19]. Thus, the interesting question that arises is: when do a NP and an oscillating dipole behave in a similar way under tight illumination?

The dashed-dotted lines in Figure 1(a) and 1(b) show $\mathcal{K}_{\rm sca}$ of a resonant point-like dipole for the focusing angle $\alpha = 90^\circ$. Also in this case, $\mathcal{K}_{\rm sca}$, which we call $\mathcal{K}_{\rm dp}$ for a point-like dipole, is a function of α and reads

$$\mathcal{K}_{\rm dp} = \frac{128}{75}\frac{1}{\sin^2\alpha}\left[1 - \frac{1}{8}(5 + 3\cos\alpha)\cos^{3/2}\alpha\right]^2. \tag{8}$$

This value is independent of the dipole resonant wavelength and for $\alpha = 90^\circ$ reaches the maximum value of $\mathcal{K}_{\rm dp} \simeq 1.707$ [1]. As depicted in Figure 1(b), a 100 nm silver NP in water exhibits a $\mathcal{K}_{\rm sca}$ very close to $\mathcal{K}_{\rm dp}$ on its dipole resonance. It could also be seen that a 100 nm gold NP does not approach the scattering ratio of a perfect radiator as well, because of the higher material losses.

2.3 Transmission, reflection and absorption

The scattering $\mathcal{K}_{\rm sca}$ and absorption $\mathcal{K}_{\rm abs}$ ratios determine the conversion of the incident power into the corresponding quantities. Nevertheless, they give no information about the directionality of the scattered field. By investigating the transmission and reflection of a beam interacting with a nano-object a better understanding of the process is obtained. The simplest and most commonly discussed case is that of a plane incident wave [19, 27]. If the power is only collected along the z axis, the transmission is expressed as

$$T = \frac{I}{I_{\rm inc}} = 1 - \frac{\sigma}{\mathcal{A}}, \tag{9}$$

where I and $I_{\rm inc}$ are the transmitted and incident intensities, respectively. $\mathcal{A}$ is the beam cross sectional area, and σ is the extinction cross section. The ratio $\sigma/\mathcal{A}$ represents the fraction of the power removed from the incident beam. The optical theorem states that the interference term $P_{\rm s+a}$ in Eq. (5) depends only on the scattered field in the forward direction. It can thus be shown that $P_{\rm s+a} = I_{\rm inc}\sigma$ and the term $P_{\rm s+a}$ is commonly referred to as the "extinguished" power [19]. Note that if the off-axis collection is included, a fraction of the scattered power must be added to Eq. (9).

For focused illumination the intensity is not homogeneous and the optical theorem no longer holds [25]. In fact, $P_{\rm s+a}$ is not all concentrated along the z axis, but it covers a range of angles from $\beta = 0^\circ$ to $\beta = \alpha$. Thus, $P_{\rm s+a}$ does not correspond to the power removed from the beam in a transmission experiment. For this reason, we do not equate $P_{\rm s+a}$ with the extinguished power, although this convention can be found in the literature [16, 25]. If the collection angle is extended to the forward hemisphere, i.e. $\beta = 90^\circ$, the transmission (T) through an ideal dipole can be nevertheless formulated in terms of the ratio of powers as [1]

$$T = \frac{P}{P_{\rm inc}} = 1 - \frac{1}{2}\mathcal{K}_{\rm dp}, \tag{10}$$

where P is the transmitted power.

In the case of a dissipating dipole, absorption also plays a major role in the amount of light that gets transmitted and the generalized formula for tightly focused beams becomes

$$T = 1 + \frac{1}{2}\mathcal{K}_{\rm sca} - \mathcal{K}_{\rm s+a} = 1 - \frac{1}{2}\mathcal{K}_{\rm sca} - \mathcal{K}_{\rm abs}. \tag{11}$$

Moreover, scattering and absorption have a different weight, because half of the scattered power is added to the incident power in the forward direction, while $\mathcal{K}_{\rm s+a}$ contributes with a negative sign. Eq. (11) tells us that the correct definition of extinction for tight illumination, i.e. the fraction of power removed in the forward direction, is $\mathcal{K}_{\rm abs} + \mathcal{K}_{\rm sca}/2$. However, when the power is collected with an angle $\beta < 90^\circ$ the above expressions have a more complicated form [1]. Furthermore, Eq. (11) is not valid for a non-dipolar scatterer, because $P_{\rm sca}$ is not equally distributed in the forward and backward directions. Consequently, we compute the transmission through metal NPs by integrating the Poynting vector of the total field in the forward hemisphere ($\beta = 90^\circ$). Reflection (R) is given by integrating the Poynting vector of the scattered field in the backward hemisphere or alternatively by $R = 1 - T - \mathcal{K}_{\rm abs}$.

Figure 2 displays the transmission spectrum for various metal NPs. We note that a 100 nm silver NP exhibits almost the same transmission dip of a point-like oscillating dipole when excited at the dipole resonance. The latter is indicated by a

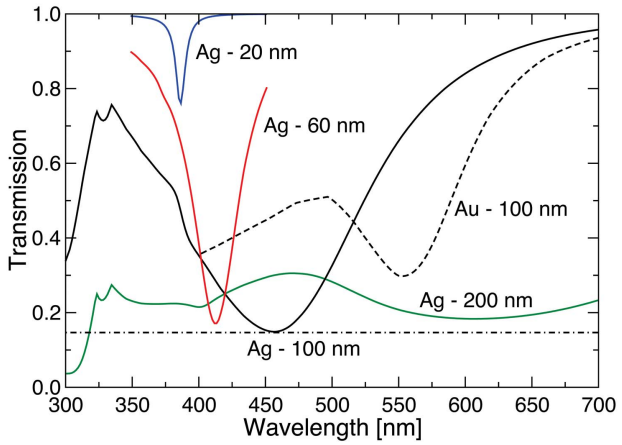

FIG. 2 Transmission ($\beta = 90°$) for silver and gold NPs in water ($n_b = 1.3$) under a FPW ($\alpha = 90°$). The curve labels indicate the NP composition and size. The dashed-dotted line refers to the transmission for a resonant point-like oscillating dipole under the same illumination conditions [1].

dashed-dotted line and corresponds to the value given by Eq. (10). Indeed, as shown in Figure 1, because $\mathcal{K}_{sca} \simeq \mathcal{K}_{dp}$ and $\mathcal{K}_{abs} \ll \mathcal{K}_{sca}$, Eqs. (10) and (11) shall yield almost the same result. Even if the dip is very close to that of a point-like oscillating dipole, the transmission spectrum of the 100 nm silver NP is not as simple as a Lorentzian profile [1]. The reason is that the NP supports a quadrupole resonance around 380 nm and the dipolar polarizability of the NP includes material dispersion [28] and depolarization effects [26]. In fact, smaller silver NPs yield a transmission spectrum that is closer to that of a dipolar radiator, but the dip is smaller because absorption reduces the strength of the polarizability on resonance. For the same reason a 100 nm gold NP yields a transmission larger than a perfect radiator.

On the other hand, larger metal NPs support higher-order resonances that spectrally overlap and, for this reason, exhibit a more complex scattering pattern. More precisely, because P_{sca} is not equally distributed in the forward and backward directions, Eq. (11) is not valid. Indeed, Figure 2 shows that for a 200 nm silver NP the transmission spectrum does not resemble a Lorentzian profile and, at the dipolar resonance ($\lambda \simeq 600$ nm), the dip is less pronounced than for a 100 nm silver NP ($\lambda \simeq 455$ nm).

2.4 Discussion

To better understand how close a metal NP to a point-like oscillating dipole is, we consider the transmission dip and the reflection peak as a function of the NP size. While for silver NPs the transmission dip and the reflection peak occur at the same wavelength, for gold NPs there is a small shift due to the fact that the plasmon-polariton resonance crosses the onset of interband transitions [28], which gives a rapid increase of losses and hence reshapes the transmission profile. Figure 3(a) and 3(b) respectively show the results for gold and silver NPs. The dashed-dotted lines refer to the maximal reflection and transmission for an oscillating dipole [1]. We find that a gold NP approaches a dipolar radiator when its diameter is larger than 160 nm and that above 180 nm the transmission dip starts to increase because of the spectral overlap with higher-order

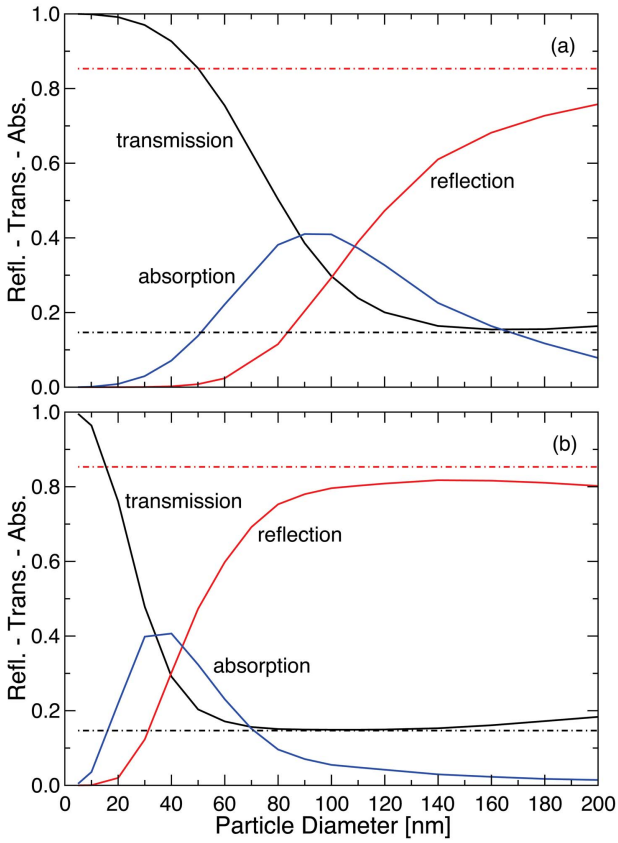

FIG. 3 Transmission, reflection and absorption $\mathcal{K}_{abs}$ for (a) gold and (b) silver NPs in water ($n_b = 1.3$) under a FPW ($\alpha = 90°$) as a function of the NP size. The dashed-dotted lines refer to transmission and reflection for a resonant point-like oscillating dipole under the same illumination conditions [1].

modes. On the contrary, a silver NP reaches the properties of an ideal oscillating dipole already for diameters as small as 70 nm.

We would like to stress that the transmission dip is not enough to judge how close the NP is to a dipolar radiator model. That is because the transmission dip contains also the effect of absorption, as shown in Eq. (11), while the reflection only provides information on scattering. Indeed we find that even when the transmission dip is close to the limit of a perfect radiator, $\mathcal{K}_{abs}$ is still significant. It is also interesting to see that for a silver NP $\mathcal{K}_{abs}$ is maximal when the diameter is about 40 nm, while for gold when it is about 90 nm. While it is commonly assumed that very small NPs are light absorbers, one has to keep in mind that the efficiency of the process goes down (see Figure 3). For the purpose of converting a certain amount of input power into heat, one sees that the highest efficiency is met when scattering is not small. In addition, when the NP diameter is smaller than about 20 nm for silver NPs and 60 nm for gold NPs, the detection signal is stronger if one measures the transmission dip or equally the absorbed power [11]. Indeed, transmission and absorption give exactly the same contrast because the scattered power is negligible and Eq. (11) becomes $T = 1 - \mathcal{K}_{abs}$. For instance, for very small diameters such as 5 nm, a silver and a gold NP would respectively exhibit a contrast of $\simeq 0.45\%$ and $\simeq 0.013\%$.

To further investigate how a metal NP mimics a point-like radiator, we focus our attention on a 100 nm silver NP and ex-

amine the transmission dip and reflection peak as a function of the focusing angle. The excitation wavelength is fixed to the dipole resonance. Figure 4 compares these two quantities with the values obtained for an ideal oscillating dipole [1]. The agreement is very good over a broad range of focusing angles. The maximum deviation of the reflection curves is at $\alpha = 90°$, where it reaches about 6%. This shows that more energy goes into absorption when focusing more tightly.

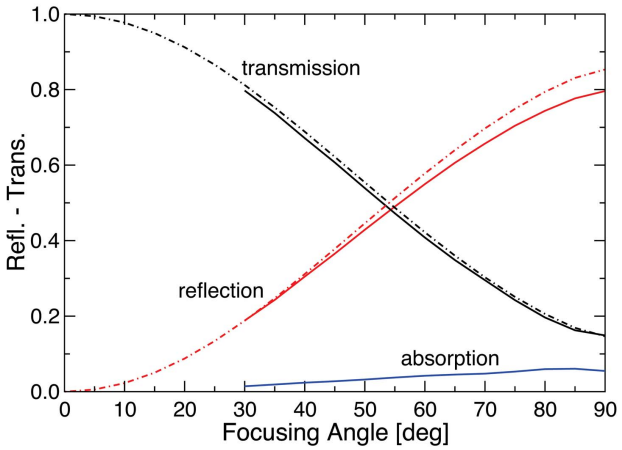

FIG. 4 Transmission, reflection and absorption $\mathcal{K}_{\text{abs}}$ for a 100 nm silver NP in water ($n_{\text{b}} = 1.3$) under a FPW as a function of the focusing angle α. The dashed-dotted lines refer to transmission and reflection for a resonant point-like oscillating dipole under the same illumination conditions [1].

3 CONCLUSIONS

We studied the scattering properties of spherical silver and gold NPs illuminated by a FPW and compared them with the response of an ideal oscillating dipole. We have described this process by introducing the scattering, and absorption ratios. These quantities are different from the well known scattering and absorption efficiencies for plane wave illumination [19] as well as those defined for a Gaussian beam [29]. We have also seen that the maximal $\mathcal{K}_{\text{abs}}$ for silver and gold NPs respectively occurs for diameters of 40 nm and 90 nm. These results are relevant for applications that exploit the heating created by the metal NP, such as in cancer therapy [30], laser ablation and optical data storage [31].

When the response of the metal NP can be described by a dipolar polarizability, Eq. (11) relates the transmission to the scattered and absorbed powers. With that one can have a quantitative estimate of the signal from metal NPs [7]–[11] and also other nano-objects like colloidal quantum dots and viruses [12, 18].

It was shown that a 100 nm silver NP behaves to a very good approximation like a point-like radiator. This suggests that such NPs could be used for fundamental experiments where quantum emitters are replaced by classical oscillating dipoles. These include studies on the van der Waals-Casimir interactions [20], and on the extinction properties of emitters [15]. In the latter case, one could investigate improved focusing systems, such as directional dipole waves [1] and perform simpler test experiments at room temperature with metal NPs instead of quantum emitters at cryogenic temperatures [15]. Furthermore, one could study the coupling of single photons to a plasmon-polariton mode [32] with a large efficiency at room temperature. Finally, our results may find application also in the area of ultrafast phenomena and coherent control [33, 34], where the interaction of the incoming beam with the system plays a critical role.

Acknowledgments

This work was supported by the ETH Zurich research grant TH-49/06-1.

References

[1] G. Zumofen, N. M. Mojarad, V. Sandoghdar, and M. Agio, "Perfect Reflection of Light by an Oscillating Dipole" Phys. Rev. Lett. **101**, 180404 (2008).

[2] S. J. van Enk, "Atoms, dipole waves, and strongly focused light beams" Phys. Rev. A **69**, 043813 (2004).

[3] N. M. Mojarad, V. Sandoghdar, and M. Agio, "Plasmon spectra of nanospheres under a tightly focused beam" J. Opt. Soc. Am. B **25**, 651–658 (2008).

[4] J. Lermé, G. Bachelier, P. Billaud, C. Bonnet, M. Broyer, E. Cottancin, S. Marhaba, and M. Pellarin, "Optical response of a single spherical particle in a tightly focused light beam: application to the spatial modulation spectroscopy technique" J. Opt. Soc. Am. A **25**, 493–514 (2008).

[5] D. Pinotsi and A. Imamoğlu, "Single Photon Absorption by a Single Quantum Emitter" Phys. Rev. Lett. **100**, 093603 (2008).

[6] M. Stobińska, A. Gernot, and G. Leuchs, "Perfect excitation of a matter qubit by a single photon in free space" arXiv:0808.1666v1 (2008).

[7] C. Sönnichsen, S. Geier, N. E. Hecker, G. von Plessen, J. Feldmann, H. Ditlbacher, B. Lamprecht, J. R. Krenn, F. R. Aussenegg, V. Z.-H. Chan, J. P. Spatz, and M. Möller, "Spectroscopy of single metallic nanoparticles using total internal reflection microscopy" Appl. Phys. Lett. **77**, 2949–2951 (2000).

[8] D. Boyer, P. Tamarat, A. Maali, B. Lounis, and M. Orrit, "Photothermal Imaging of Nanometer-Sized Metal Particles Among Scatterers" Science **297**, 1160–1163 (2002).

[9] K. Lindfors, T. Kalkbrenner, P. Stoller, and V. Sandoghdar, "Detection and Spectroscopy of Gold Nanoparticles Using Supercontinuum White Light Confocal Microscopy" Phys. Rev. Lett. **93**, 037401 (2004).

[10] A. Arbouet, D. Christofilos, N. Del Fatti, F. Vallée, J. R. Huntzinger, L. Arnaud, P. Billaud, and M. Broyer, "Direct Measurement of the Single-Metal-Cluster Optical Absorption" Phys. Rev. Lett. **93**, 127401 (2004).

[11] S. Berciaud, L. Cognet, G. A. Blab, and B. Lounis, "Photothermal Heterodyne Imaging of Individual Nonfluorescent Nanoclusters and Nanocrystals" Phys. Rev. Lett. **93**, 257402 (2004).

[12] H. Ewers, V. Jacobsen, E. Klotzsch, A. E. Smith, A. Helenius, and V. Sandoghdar, "Label-Free Optical Detection and Tracking of Single Virions Bound to Their Receptors in Supported Membrane Bilayers" Nano Lett. **7**, 2263–2266 (2007).

[13] B. D. Gerardot, S. Seidl, P. A. Dalgarno, R. J. Warburton, M. Kroner, K. Karrai, A. Badolato, and P. M. Petroff, "Contrast in transmission

spectroscopy of a single quantum dot" Appl. Phys. Lett. **90**, 221106 (2007).

[14] A. N. Vamivakas, M. Atatüre, J. Dreiser, S. T. Yilmaz, A. Badolato, A. K. Swan, B. B. Goldberg, A. Imamoğlu, and M. S. Ünlü, "Strong Extinction of a Far-Field Laser Beam by a Single Quantum Dot" Nano Lett. **7**, 2892–2896 (2007).

[15] G. Wrigge, I. Gerhardt, J. Hwang, G. Zumofen, and V. Sandoghdar, "Efficient coupling of photons to a single molecule and the observation of its resonance fluorescence" Nat. Phys. **4**, 60–66 (2008).

[16] G. Wrigge, J. Hwang, I. Gehardt, G. Zumofen, and V. Sandoghdar, "Exploring the limits of single emitter detection in fluorescence and extinction" Opt. Express **16**, 17358–17365 (2008).

[17] M. K. Tey, Z. Chen, S. A. Aljunid, B. Chng, F. Huber, G. Maslennikov, and C. Kurtsiefer, "Strong interaction between light and a single trapped atom without the need for a cavity" Nat. Phys. **4**, 924–927 (2008).

[18] P. Kukura, M. Celebrano, A. Renn, and V. Sandoghdar, "Imaging a Single Quantum Dot When It Is Dark" Nano Lett. **9**, 926–929 (2009).

[19] C. Bohren and D. Huffman, *Absorption and Scattering of Light by Small Particles* (John Wiley & Sons, New York, 1983).

[20] U. Håkanson, M. Agio, S. Kühn, L. Rogobete, T. Kalkbrenner, and V. Sandoghdar, "Coupling of plasmonic nanoparticles to their environments in the context of van der Waals–Casimir interactions" Phys. Rev. B **77**, 155408 (2008).

[21] T. Kalkbrenner, U. Håkanson, A. Schädle, S. Burger, C. Henkel, and V. Sandoghdar, "Optical Microscopy via Spectral Modifications of a Nanoantenna" Phys. Rev. Lett. **95**, 200801 (2005).

[22] N. M. Mojarad and M. Agio, "Tailoring the excitation of localized surface plasmon-polariton resonances by focusing radially-polarized beams" Opt. Express **17**, 117–122 (2009).

[23] B. Richards and E. Wolf, "Electromagnetic Diffraction in Optical Systems. II. Structure of the Image Field in an Aplanatic System" P. Roy. Soc. A. - Math. Phys. **253**, 358–379 (1959).

[24] C. Sheppard and P. Török, "Efficient calculation of electromagnetic diffraction in optical systems using a multipole expansion", J. Mod. Optic. **44**, 803–818 (1997).

[25] J. A. Lock, J. T. Hodges, and G. Gouesbet, "Failure of the optical theorem for Gaussian-beam scattering by a spherical particle" J. Opt. Soc. Am. A **12**, 2708–2715 (1995).

[26] M. Meier and A. Wokaun, "Enhanced fields on large metal particles: dynamic depolarization" Opt. Lett. **8**, 581–583 (1983).

[27] J. Jackson, *Classical Electrodynamics*, third edn. (John Wiley & Sons, New York, 1999).

[28] P. B. Johnson and R. W. Christy, "Optical Constants of the Noble Metals" Phys. Rev. B **6**, 4370–4379 (1972).

[29] J. A. Lock, "Interpretation of extinction in Gaussian-beam scattering" J. Opt. Soc. Am. A **12**, 929–938 (1995).

[30] X. Huang, P. Jain, I. El-Sayed, and M. El-Sayed, "Plasmonic photothermal therapy (PPTT) using gold nanoparticles" Laser. Med. Sci. **23**, 217–228 (2008).

[31] M. Sugiyama, S. Inasawa, S. Koda, T. Hirose, T. Yonekawa, T. Omatsu, and A. Takami, "Optical recording media using laser-induced size reduction of Au nanoparticles" Appl. Phys. Lett. **79**, 1528–1530 (2001).

[32] M. S. Tame, C. Lee, J. Lee, D. Ballester, M. Paternostro, A. V. Zayats, and M. S. Kim, "Single-Photon Excitation of Surface Plasmon Polaritons" Phys. Rev. Lett. **101**, 190504 (2008).

[33] M. Aeschlimann, M. Bauer, D. Bayer, T. Brixner, F. J. Garcia de Abajo, W. Pfeiffer, M. Rohmer, C. Spindler, and F. Steeb, "Adaptive subwavelength control of nano-optical fields" Nature **446**, 301–304 (2007).

[34] M. I. Stockman, M. F. Kling, U. Kleineberg, and F. Krausz, "Attosecond nanoplasmonic-field microscope" Nat. Photonics **1**, 539–544 (2007).